Crystal structure of ceftriaxone sodium hemiheptahydrate, $C_{18}H_{16}N_8O_7S_3Na_2(H_2O)_{3.5}$

Diana Gonzalez,[1] Joseph T. Golab,[1] Jan Y. Eilert,[2] Rong Wang,[2] and James A. Kaduk [2,3,a)]
[1]*Illinois Mathematics and Science Academy, 1500 Sullivan Rd., Aurora 60506-1000, Illinois, USA*
[2]*Illinois Institute of Technology, 3101 S. Dearborn St., Chicago 60616, Illinois, USA*
[3]*North Central College, 131 S. Loomis St., Naperville 60540, Illinois, USA*

(Received 2 April 2020; accepted 13 April 2020)

The crystal structure of ceftriaxone sodium hemiheptahydrate has been solved and refined using synchrotron X-ray powder diffraction data and optimized using density functional techniques. Ceftriaxone sodium hemiheptahydrate crystallizes in the space group $C2$ (#5) with $a = 30.56\ 492\ (16)$, $b = 4.75\ 264(2)$, $c = 18.54\ 978(16)$ Å, $\beta = 90.3545(6)$, $V = 2694.562(21)$ Å^3, and $Z = 4$. Both Na exhibit trigonal bipyramidal coordination. Prominent in the structure are alternating Na/O and organic layers perpendicular to the c-axis. There are many O–H···O hydrogen bonds involving the water molecules and the ionized portions of the anion. There are a surprising number of C–H···S hydrogen bonds, as well as C–H···N and C–H···O hydrogen bonds. The powder pattern has been submitted to ICDD for inclusion in the Powder Diffraction File™. © *2020 International Centre for Diffraction Data*. [doi:10.1017/S0885715620000299]

Key words: ceftriaxone sodium, Rocephin, powder diffraction, Rietveld refinement, density functional theory

I. INTRODUCTION

Ceftriaxone sodium hemiheptahydrate (brand names Rocephin, Lendacin, and Longaceph) is a drug classified as a cephalosporin, a bacterial beta-lactam antibiotic that binds to penicillin-binding proteins (PBP). Bacterial infections treated by sodium ceftriaxone include meningitis, lower respiratory tract infections, and urinary tract infections. This drug is commonly administered via IV or injection into the muscle and is only prescribed to prevent susceptible bacteria. The IUPAC name (CAS Registry number 104376-79-6) is sodium 3-(((6R,7R)-7-((Z)-2-(2-aminothiazol-4-yl)-2-(methoxyimino) acetamido)-2-carboxylato-8-oxo-5-thia-1-azabicyclo[4.2.0]oct-2-en-3-yl)methylthio)-2-methyl-5,6-dioxo-5,6-dihydro-2H-1,2,4-triazin-1-ide hemiheptahydrate. A two-dimensional molecular diagram is shown in Figure 1.

A powder pattern of ceftriaxone sodium hemiheptahydrate is reported in Zhang *et al*. (2005). The same pattern is reproduced in Chinese Patent CN 102875574A (Yang *et al*., 2012) as an example of the prior art. The space group of ceftriaxone sodium is claimed to be $P2_1/c$ in Wang *et al*. (2007), but this is not possible for a chiral molecule such as ceftriaxone.

This work was carried out as part of a project (Kaduk *et al*., 2014) to determine the crystal structures of large-volume commercial pharmaceuticals and include high-quality powder diffraction data for these pharmaceuticals in the Powder Diffraction File (Gates-Rector and Blanton, 2019).

II. EXPERIMENTAL

Ceftriaxone sodium hemiheptahydrate was a commercial reagent, USP grade (Baxter plant released for API use), and was used as-received. The white powder was packed into a 1.5-mm-diameter Kapton capillary and rotated during the measurement at ~50 Hz. The powder pattern was measured at 295 K at beamline 11-BM (Lee *et al*., 2008; Wang *et al*., 2008) of the Advanced Photon Source at Argonne National Laboratory using a wavelength of 0.412 703 Å from 0.5 to 50° 2θ with a step size of 0.001° and a counting time of 0.1 s step^{-1}.

The pattern was indexed on a monoclinic unit cell with $a = 30.5756$, $b = 4.7536$, $c = 18.5557$ Å, $\beta = 90.3526$, $V = 2696.91$ Å^3, and $Z = 4$ using DICVOL14 (Louër and Boultif, 2014). Analysis of the systematic absences using EXPO2014 (Altomare *et al*., 2013) indicated the space group $C2$, which was confirmed by the successful solution and refinement of the structure. A reduced cell search in the Cambridge Structural Database (Groom *et al*., 2016) yielded two hits, but no structures for ceftriaxone derivatives. A ceftriaxone anion was built using Spartan '18 (Wavefunction, 2018) and converted into .mol2 and .mop files using OpenBabel (O'Boyle *et al*., 2011). The structure was solved using Monte Carlo simulated annealing techniques as implemented in EXPO. A ceftriaxone anion, two Na, and four O (water molecules) were used as fragments with 010 preferred orientation and a bump penalty.

Rietveld refinement was carried out using GSAS-II (Toby and Von Dreele, 2013). Only the 1.0–22.0° portion of the pattern was included in the refinement ($d_{min} = 1.084$ Å). All non-H bond distances and angles in the anion were subjected to restraints, based on a Mercury/Mogul Geometry Check (Bruno *et al*., 2004; Sykes *et al*., 2011) of the molecule. The Na-ligand bonds were not restrained. The results were

a)Author to whom correspondence should be addressed. Electronic mail: kaduk@polycrystallography.com

 0885-7156/2020/35(3)/206/7/$18.00

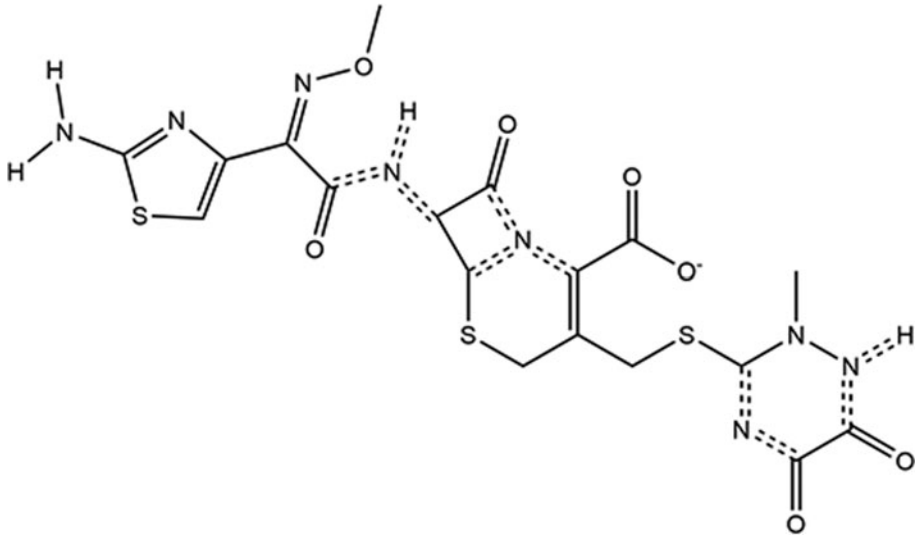

Figure 1. The molecular structure of the ceftriaxone dianion.

exported to a .csv file. The Mogul average and standard deviation for each quantity were used as the restraint parameters and were incorporated using the new feature Restraints/Edit Restraints/Add MOGUL Restraints, which reads the bond distance and angle restraints from the .csv file. The restraints contributed 4.3% to the final χ^2. The hydrogen atoms were included in calculated positions, which were recalculated during the refinement using Materials Studio (Dassault Systèmes, 2018). The positions of the active hydrogen atoms were deduced by analysis of potential hydrogen bonding patterns. The U_{iso} of the non-H atoms were grouped by chemical similarity. A common U_{iso} was refined for the atoms of the pyridine ring, the fused ring system, the thiazole ring, the substituents, the two Na, four water molecules, and the S atoms. The U_{iso} for each hydrogen atom was constrained to be 1.3× that of the heavy atom to which it is attached. In the initial refinement, the water molecule oxygen atoms refined to unreasonable positions, so they were removed from the model. Exploring voids using Mercury (probe radius = 1.2 Å) indicated a void at a ½, 0.45, ½, which was assigned to O41. Decreasing the probe radius yielded two additional voids, which were assigned as O42 and O39. Decreasing the radius further to 0.9 Å yielded another void, which was O65. The background was modeled using a 6-term shifted Chebyshev polynomial, and a peak at 5.23° to model the scattering from the Kapton capillary and any amorphous component.

The final refinement of 161 variables using 21 034 observations and 96 restraints yielded the residuals $R_{wp} = 0.06\,336$ and GOF = 1.37. The largest peak (0.462 Å from C3) and hole (3.076 Å from O29) in the difference Fourier map were 0.198 and $-0.210(52)\ e\text{Å}^{-3}$. The Rietveld plot is included in Figure 2. The largest errors in the fit are in the intensities of

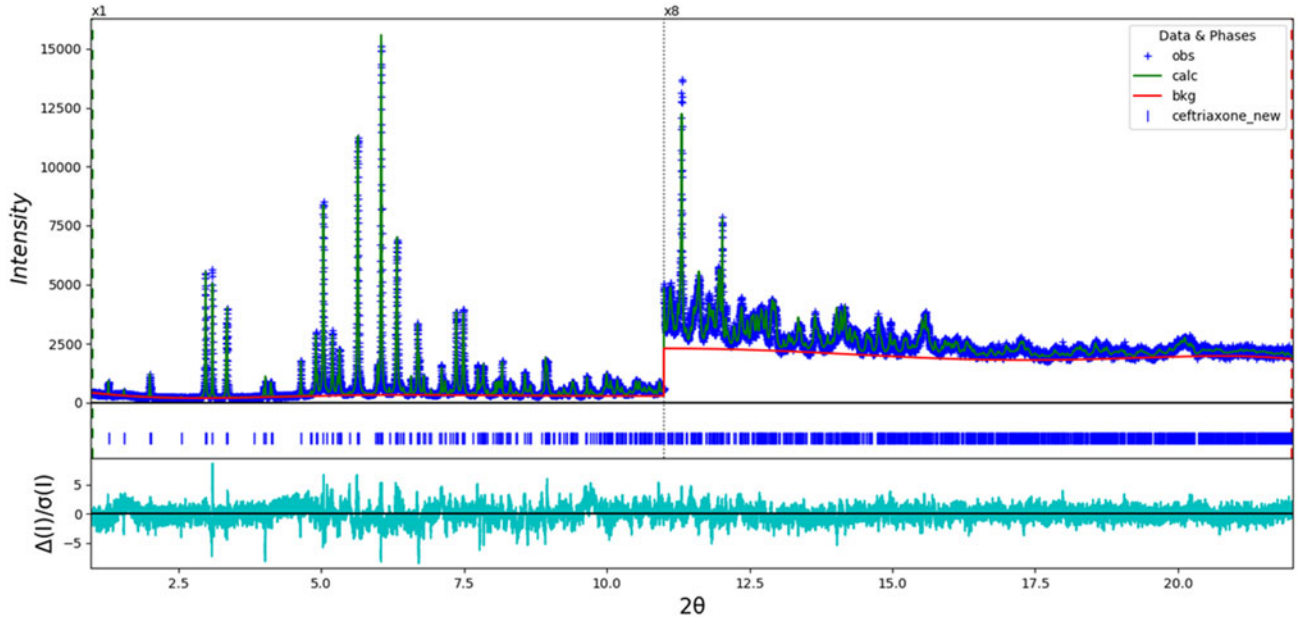

Figure 2. The Rietveld plot for the refinement of ceftriaxone sodium hemiheptahydrate. The blue crosses represent the observed data points, and the green line is the calculated pattern. The cyan curve is the normalized error plot. The vertical scale has been multiplied by a factor of 8× for $2\theta > 11.0°$.

https://doi.org/10.1017/S0885715620000299 Published online by Cambridge University Press

some of the peaks, and small position errors which may represent a change of the specimen in the beam.

A density functional geometry optimization was carried out using VASP (Kresse and Furthmüller, 1996) through the MedeA graphical interface (Materials Design, 2016). The calculation was carried out on 16 2.4 GHz processors (each with 4 GB RAM) of a 64-processor HP Proliant DL580 Generation 7 Linux cluster at North Central College. The calculation used the GGA-PBE functional, a plane wave cutoff energy of 400.0 eV, and a *k*-point spacing of 0.5 $Å^{-1}$ leading to a 6 × 6 × 1 mesh, and took ~194 h. A fixed point density functional geometry calculation was carried out using CRYSTAL14 (Dovesi *et al*., 2014). The basis sets for the H, C, N, and O atoms were those of Gatti *et al*. (1994), and the basis sets for S and Na were those of Peintinger *et al*. (2013). The calculation was run on eight 2.1 GHz Xeon cores (each with 6 GB RAM) of a 304-core Dell Linux cluster at IIT, using 8 *k*-points and the B3LYP functional, and took 1 h.

III. RESULTS AND DISCUSSION

The powder pattern of the ceftriaxone sodium hemiheptahydrate studied here matches that of Zhang *et al*. (2005) well enough to conclude that the two materials are the same, and that our sample is representative (Figure 3).

The refined atom coordinates of ceftriaxone sodium hemiheptahydrate and the coordinates from the density functional theory (DFT) optimization have been deposited with ICDD. The root-mean-square (rms) Cartesian displacement of the non-hydrogen atoms in the Rietveld-refined and the DFT-optimized structures of the anion is 0.19 Å (Figure 4). The good agreement between the refined and optimized structures suggests that the structure is correct (van de Streek and Neumann, 2014). This discussion concentrates on the VASP-optimized structure. The asymmetric unit (with atom numbering) is illustrated in Figure 5, and the crystal structure is presented in Figure 6.

Both Na37 and Na38 are 5-coordinate (trigonal bipyramidal). Na37 is bound to O18, two O20 (carbonyl), and two water molecules O45 and O65. Na38 is coordinated to the ionized carboxylate O11 and O12, O18, and the two water molecules O39 and O41. The bond valence sums of Na37 and Na38 are 1.10 and 0.98, respectively. The Mulliken overlap populations (~0.05 *e*) indicate that the Na–O bonds have a significant covalent character. Main features of the structure are alternating Na/O and organic layers perpendicular to the *c*-axis. The hydrogen bonds are part of these Na/O layers.

Most of the bond distances, bond angles, and torsion angles in the anions fall within the normal ranges indicated by a Mercury/Mogul Geometry Check (Macrae *et al*., 2008). The C17–O18 bond distance of 1.286 Å (average = 1.236 (16), *Z*-score = 3.2) and the C17–C19 bond distance of 1.422 Å (average = 1.348(11), *Z*-score = 6.5) are flagged as unusual. The C15–N16–C17 angle of 119.4° (average = 113.1(12), *Z*-score = 5.3) and the C23–N22–C15 angle of 125.9° (average = 120.6(17), *Z*-score = 3.1) are flagged as unusual. All of these occur in the ionized dioxotriazine ring, which is an unusual structure. The torsion angles O11–C10–C9–N5 and O12–C10–C9–N5 lie in the tails of broad distributions; they are unusual but not unprecedented. These torsion angles reflect the orientation of the ionized carboxylate groups, which is coordinated to Na38. The C8–C13–S14–C5 torsion angle lies in a minor *trans* population of a distribution of angles mainly ~90°. This angle reflects the orientation of two parts of the anion. The C31–C27–C25–N24 and O26–C25–C27–N28 torsion angles of 114 and 118°, respectively, are more normally ~0°; these angles reflect the orientation of the thiazole ring with respect to the rest of the molecule.

Quantum chemical geometry optimization of the ceftriaxone anion with two coordinated Na cations and four coordinated water molecules (DFT/B3LYP/6-31G*/water) using GAMESS (Schmidt *et al*., 1993; Gordon and Schmidt, 2005) indicated that in the isolated neutral complex, the conformations of the carboxylate and dioxotriazine ring differed

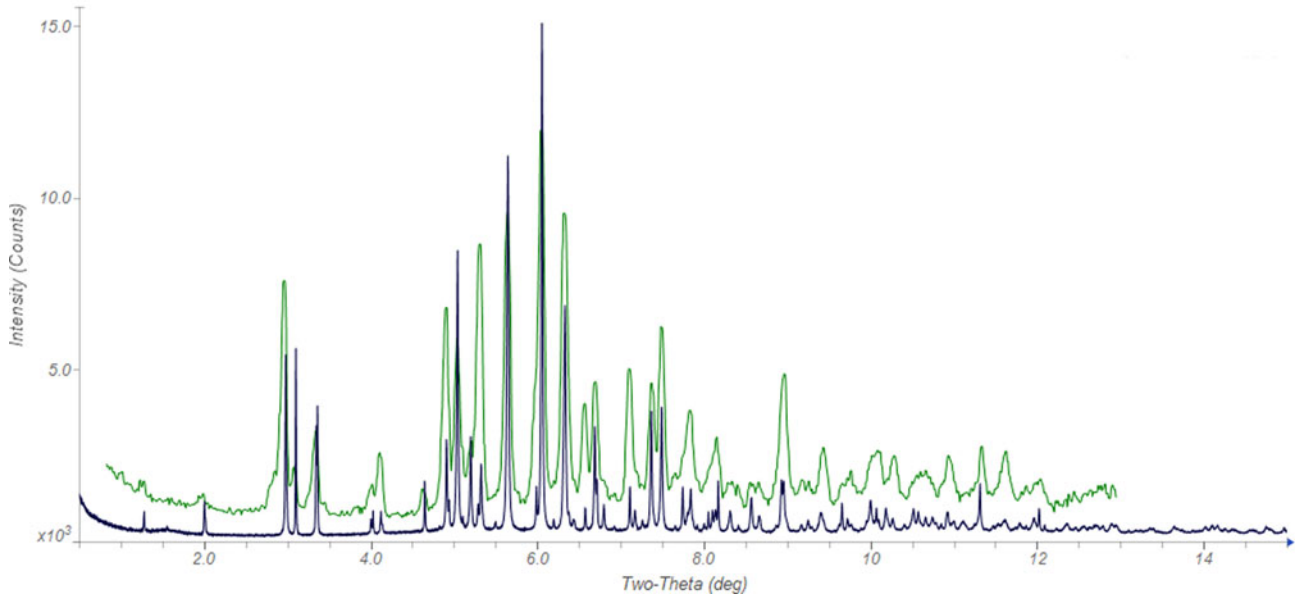

Figure 3. Comparison of the synchrotron pattern of ceftriaxone sodium hemiheptahydrate (black) to the pattern reported by Zhang *et al*. (2005) (green). The published pattern was digitized using UN-SCAN-IT (Silk Scientific, 2013) and scaled to the synchrotron wavelength of 0.412 703 Å using MDI JADE Pro (MDI, 2019).

https://doi.org/10.1017/S0885715620000299 Published online by Cambridge University Press

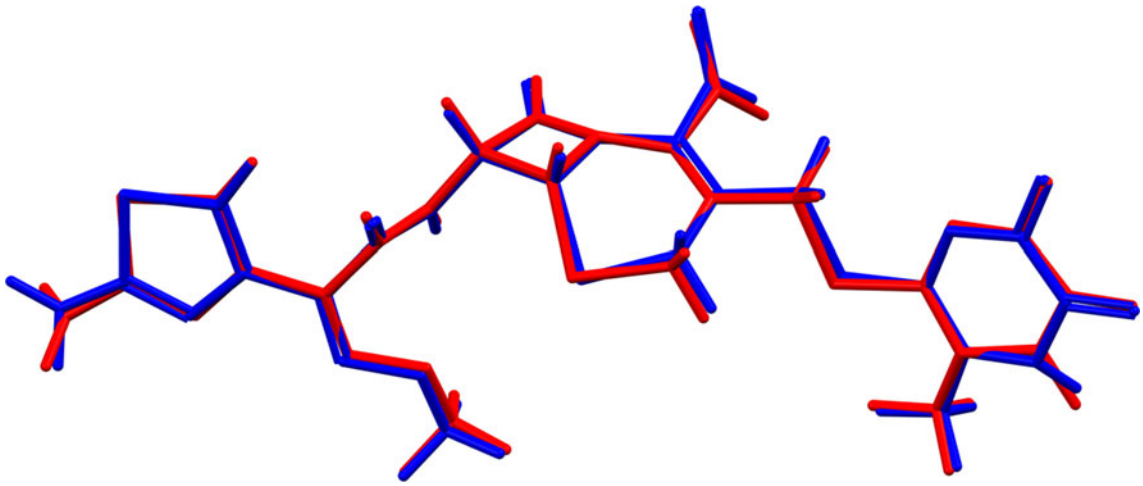

Figure 4. Comparison of the Rietveld-refined (red) and VASP-optimized (blue) structures of the anion of ceftriaxone sodium hemiheptahydrate. The rms Cartesian displacement is 0.19 Å.

from those observed in the crystal structure. In the crystal structure, each of the oxygen atoms in these groups binds to multiple Na cations, instead of the single cation in the isolated model complex. Thus, coordination to multiple cations influences the solid-state conformation. Molecular mechanics conformational analysis indicated that the minimum-energy molecular conformation is more compact than the observed one. Intermolecular interactions, thus, are important in determining the observed conformations.

Analysis of the contributions to the total crystal energy using the Forcite module of Materials Studio (Dassault, 2018) suggests that angle and torsion distortion terms are dominant in the intramolecular deformation energy, as might be expected for anions containing a fused ring system and which are coordinated to cations. The intermolecular energy is dominated by electrostatic attractions, which in this force-field based analysis include cation coordination and hydrogen bonds. The hydrogen bonds are better analyzed using the results of the DFT calculation.

Hydrogen bonds (Table I) are prominent in this structure. The water molecules O65 and O41 act as donors to the water molecules O42 and O49. Water molecules O65, O39, and O42 act as donors to the ionized carboxylate O12 and carbonyl O20. Water molecules O39 and O42 act as donors to the pyridine N16 and the carbonyl O2. The energies of the O–H–O hydrogen bonds were calculated using the correlation of Rammohan and Kaduk (2018). The amine groups N36, N24, and N21 act as donors to amine, carbonyl, and water molecules. There are a surprising number of C–H–S hydrogen bonds, as well as C–H–N and C–H–O hydrogen bonds. There is also an intramolecular C13–H48–C10 hydrogen bond to the carbon of the ionized carboxyl group.

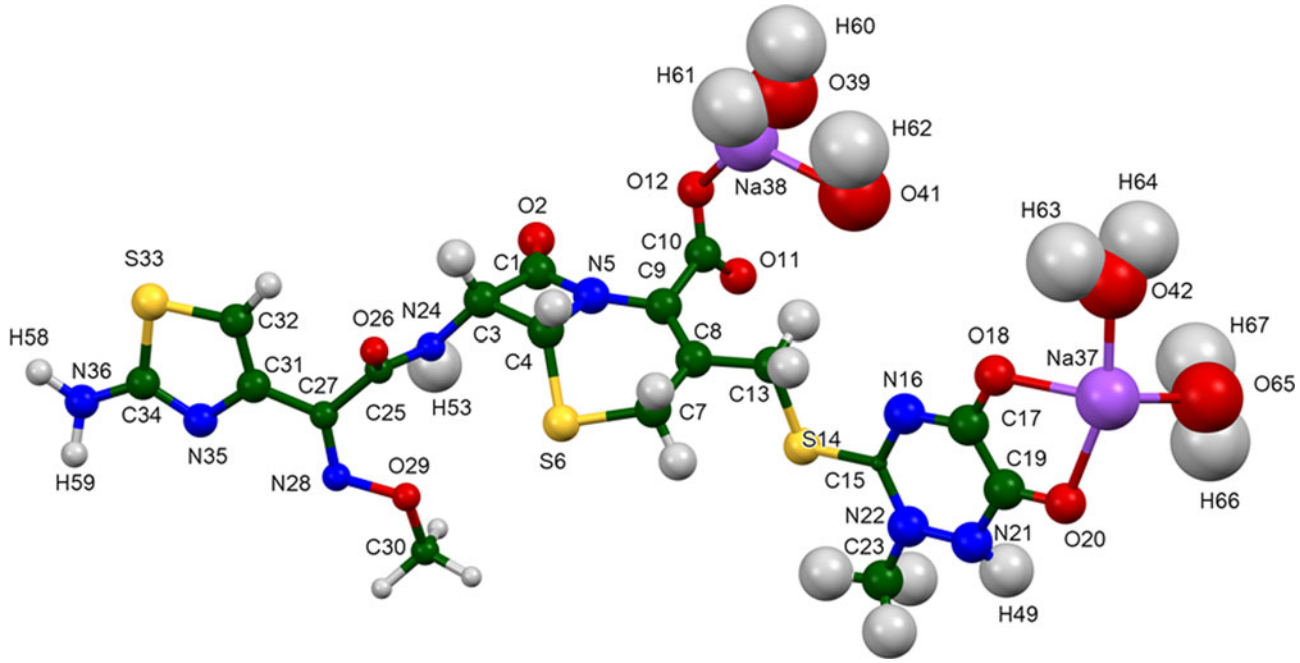

Figure 5. The asymmetric unit of ceftriaxone sodium hemiheptahydrate, with the atom numbering. The atoms are represented by 50% probability spheroids.

https://doi.org/10.1017/S0885715620000299 Published online by Cambridge University Press

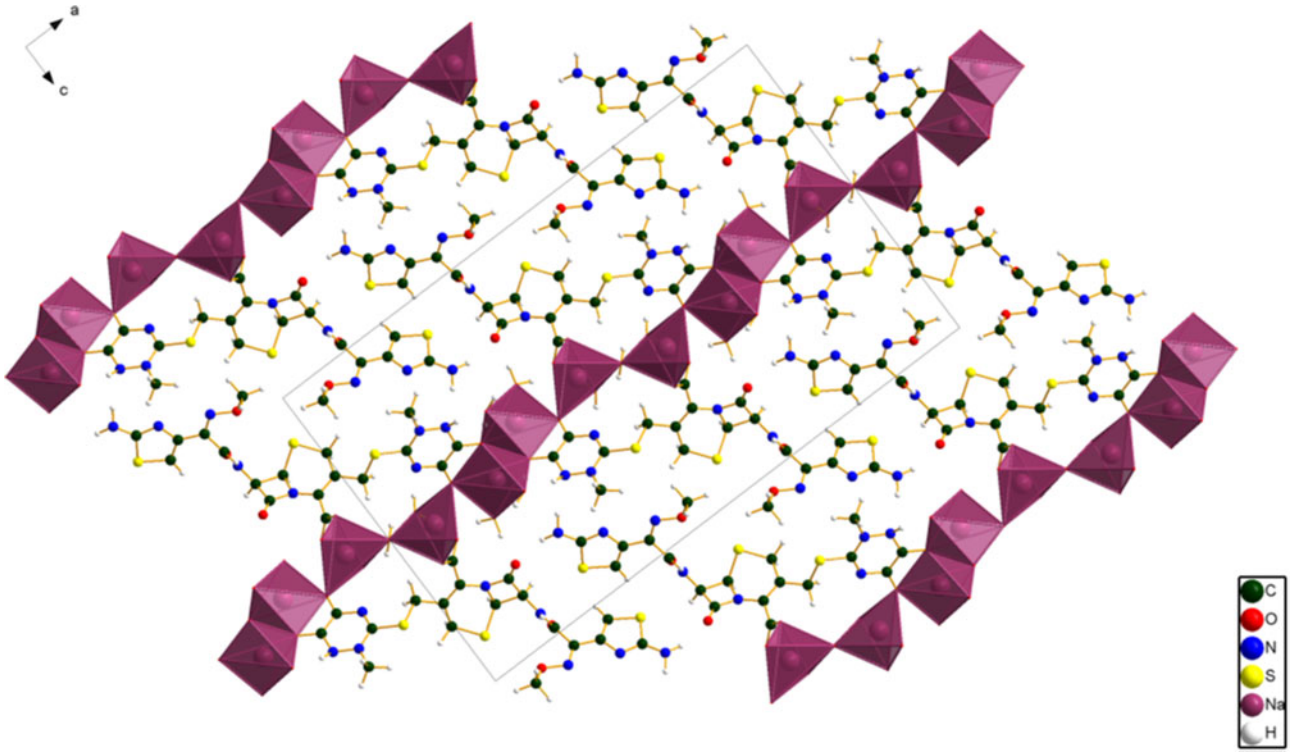

Figure 6. The crystal structure of ceftriaxone sodium hemiheptahydrate, viewed down the *b*-axis.

TABLE I. Hydrogen bonds (CRYSTAL14) in ceftriaxone sodium hemiheptahydrate.

H-bond	D–H (Å)	H···A (Å)	D···A (Å)	D–H···A (°)	Overlap (*e*)	*E* (kcal mol^{-1})
O65–H67···O42	1.992	1.811	2.746	155.7	0.061	13.5
O65–H66···O20	1.006	1.642	2.641	171.6	0.073	14.8
O41–H62···O39	.987	1.876	2.721	141.7	0.034	10.1
O39–H61···O12	0.992	1.745	2.733	173.6	0.058	13.2
O39–H60···N16	1.000	1.711	2.707	173.8	0.054	
O42–H64···O2	0.984	1.859	2.761	151.0	0.039	10.8
O42–H63···O12	0.998	1.756	2.705	157.4	0.055	12.8
N36–H59···N21	1.025	2.181	3.192	168.6	0.040	
N36–H58···O2	1.018	2.003	2.974	158.6	0.031	4.1
C32–H57···S33	1.084	2.830	3.862	159.1	0.037	
C30–H55···S6	1.096	2.886	3.558	119.7	0.015	
C30–H59···S14	1.099	2.847	3.929	168.2	0.024	
N24–H53···O26	1.033	1.761	2.778	167.7	0.063	5.8
C23–H51···N35	1.096	2.475	3.231	125.1	0.010	
C23–H50···S14	1.096	2.494[a]	2.992	106.2	0.022	
N21–H49···O65	1.043	1.862	2.852	157.1	0.058	5.6
C13–H48···C10	1.095	2.520[a]	2.987	104.4	0.011	
C13–H47···N16	1.102	2.392[a]	2.860	103.6	0.011	
C7–H46···S14	1.101	2.830[a]	3.314	106.4	0.023	
C3–H43···O2	1.100	2.403	3.257	133.2	0.013	

[a]Intramolecular.

The volume enclosed by the Hirshfeld surface (Figure 7; Hirshfeld, 1977; Turner, *et al*., 2017) is 662.57 Å^3, 98.4% of one-fourth the unit cell volume. The packing density is, thus, normal. All of the significant-close contacts (red in Figure 7) involve the hydrogen bonds. The volume/non-H atom is 16.2 Å^3.

The Bravais–Friedel–Donnay–Harker (Bravais, 1866; Friedel, 1907; Donnay and Harker, 1937) morphology suggests that we might expect needle-like morphology for ceftriaxone sodium heptahydrate, with ⟨010⟩ as the long axis. A fourth-order spherical harmonics model was included in the refinement. The texture index was 1.050, indicating that preferred orientation was significant in the rotated capillary specimen. The powder pattern of ceftriaxone sodium hemiheptahydrate from this synchrotron data set has been submitted to ICDD for inclusion in the Powder Diffraction File™.

https://doi.org/10.1017/S0885715620000299 Published online by Cambridge University Press

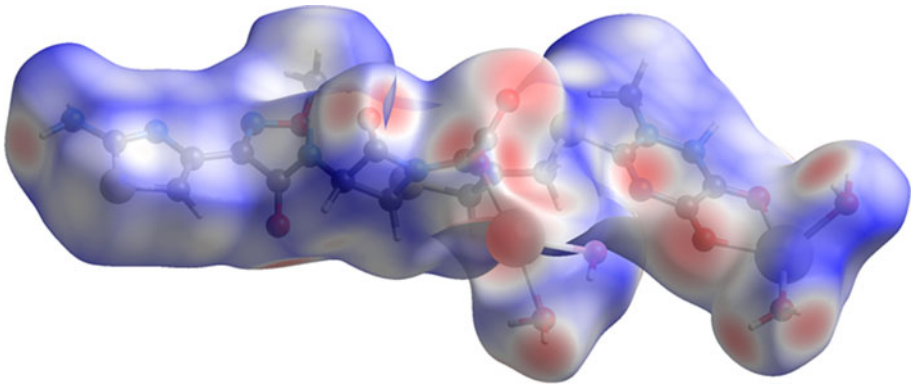

Figure 7. The Hirshfeld surface of ceftriaxone sodium hemiheptahydrate. Intermolecular contacts longer than the sums of the van der Waals radii are colored blue, and contacts shorter than the sums of the radii are colored red. Contacts equal to the sums of radii are white.

IV. DEPOSITED DATA

The Crystallographic Information Framework (CIF) files containing the results of the Rietveld refinement (including the raw data) and the DFT geometry optimization were deposited with the ICDD. You may request this data from info@icdd.com.

ACKNOWLEDGEMENTS

We thank Baxter International Inc. for the sample. Use of the Advanced Photon Source at Argonne National Laboratory was supported by the U.S. Department of Energy, Office of Science, Office of Basic Energy Sciences, under Contract No. DE-AC02-06CH11357. This work was partially supported by the International Centre for Diffraction Data. We thank Lynn Ribaud and Saul Lapidus for their assistance in the data collection, Andrey Rogachev for the use of computing resources at IIT, and Nicholas Boaz at North Central College for the thermogravimetric analysis.

CONFLICTS OF INTEREST

The authors have no conflicts of interest to declare.

Altomare, A., Cuocci, C., Giacovazzo, C., Moliterni, A., Rizzi, R., Corriero, N., and Falcicchio, A. (**2013**). "EXPO2013: a kit of tools for phasing crystal structures from powder data," J. Appl. Crystallogr. **46**, 1231–1235.

Bravais, A. (**1866**). *Etudes Cristallographiques* (Gauthier Villars, Paris).

Bruno, I. J., Cole, J. C., Kessler, M., Luo, J., Motherwell, W. D. S., Purkis, L. H., Smith, B. R., Taylor, R., Cooper, R. I., Harris, S. E., and Orpen, A. G. (**2004**). "Retrieval of crystallographically-derived molecular geometry information," J. Chem. Inf. Sci. **44**, 2133–2144.

Dassault Systèmes (**2018**). *Materials Studio 2019* (BIOVIA, San Diego, CA).

Donnay, J. D. H. and Harker, D. (**1937**). "A new law of crystal morphology extending the law of Bravais," Am. Mineral. **22**, 446–447.

Dovesi, R., Orlando, R., Erba, A., Zicovich-Wilson, C. M., Civalleri, B., Casassa, S., Maschio, L., Ferrabone, M., De La Pierre, M., D-Arco, P., Noël, Y., Causà, M., and Kirtman, B. (**2014**). "CRYSTAL14: a program for the ab initio investigation of crystalline solids," Int. J. Quantum Chem. **114**, 1287–1317.

Friedel, G. (**1907**). "Etudes sur la loi de Bravais," Bull. Soc. Fr. Mineral. **30**, 326–455.

Gates-Rector, S. and Blanton, T. (**2019**). "The Powder Diffraction File: a quality materials characterization database," Powd. Diffr. **34**(4), 352–360.

Gatti, C., Saunders, V. R., and Roetti, C. (**1994**). "Crystal-field effects on the topological properties of the electron-density in molecular crystals – the case of urea," J. Chem. Phys. **101**, 10686–10696.

Gordon, M. S. and Schmidt, M. W. (**2005**). "Advances in electronic structure theory: GAMESS a decade later," in *Theory and Applications of Computational Chemistry: The First Forty Years*, edited by C. E. Dykstra, G. Frenking, K.S. Kim, and G.E. Scuseria (Elsevier, Amsterdam), pp. 1167–1189.

Groom, C. R., Bruno, I. J., Lightfoot, M. P., and Ward, S. C. (**2016**). "The Cambridge structural database," Acta Crystallogr. B Struct. Sci. Cryst. Eng. Mater. **72**, 171–179.

Hirshfeld, F. L. (**1977**). "Bonded-atom fragments for describing molecular charge densities," Theor. Chem. Acta **44**, 129–138.

Kaduk, J. A., Crowder, C. E., Zhong, K., Fawcett, T. G., and Suchomel, M. R. (**2014**). "Crystal structure of atomoxetine hydrochloride (Strattera), $C_{17}H_{22}NOCl$," Powd. Diffr. **29**(3), 269–273.

Kresse, G., and Furthmüller, J. (**1996**). "Efficiency of ab-initio total energy calculations for metals and semiconductors using a plane-wave basis set," Comput. Mater. Sci. **6**, 15–50.

Lee, P. L., Shu, D., Ramanathan, M., Preissner, C., Wang, J., Beno, M. A., Von Dreele, R. B., Ribaud, L., Kurtz, C., Antao, S. M., Jiao, X., and Toby, B. H. (**2008**). "A twelve-analyzer detector system for high-resolution powder diffraction," J. Synchrotron Radiat. **15**(5), 427–432.

Louër, D. and Boultif, A. (**2014**). "Some further considerations in powder diffraction pattern indexing with the dichotomy method," Powd. Diffr. **29**, S7–S12.

Macrae, C. F., Bruno, I. J., Chisholm, J. A., Edington, P. R., McCabe, P., Pidcock, E., Rodriguez-Monge, L., Taylor, R., van de Streek, J., and Wood, P. A. (**2008**). "Mercury CSD 2.0 – new features for the visualization and investigation of crystal structures," J. Appl. Crystallogr. **41**, 466–470.

Materials Design (**2016**). *MedeA 2.20.4* (Materials Design Inc., Angel Fire, NM).

MDI (**2019**). *MDI JADE Pro version 7.7* (Materials Data, Livermore, CA).

O'Boyle, N., Banck, M., James, C. A., Morley, C., Vandermeersch, T., and Hutchison, G. R. (**2011**). "Open Babel: an open chemical toolbox," J. Chem. Informatics **3**, 33. doi:10.1186/1758-2946-3-33.

Peintinger, M. F., Vilela Oliveira, D., and Bredow, T. (**2013**). "Consistent Gaussian basis sets of triple-zeta valence with polarization quality for solid-state calculations," J. Comput. Chem. **34**, 451–459.

Rammohan, A. and Kaduk, J. A. (**2018**). "Crystal structures of alkali metal (Group 1) citrate salts," Acta Crystallogr. B Cryst. Eng. Mater. **74**, 239–252.

Schmidt, M. W., Baldridge, K. K., Boatz, J. A., Elbert, S. T., Gordon, M. S., Jensen, J. H., Koseki, S., Matsunaga, N., Nguyen, K. A., Su, S., Windus, T. L., Dupuis, M., and Montgomery, J. A. (**1993**). "General atomic and molecular electronic structure system," J. Comput. Chem. **14**, 1347–1363.

Silk Scientific (**2013**). *UN-SCAN-IT 7.0* (Silk Scientific Corporation, Orem, UT).

Sykes, R. A., McCabe, P., Allen, F. H., Battle, G. M., Bruno, I. J., and Wood, P. A. (**2011**). "New software for statistical analysis of Cambridge Structural Database data," J. Appl. Crystallogr. **44**, 882–886.

Toby, B. H. and Von Dreele, R. B. (**2013**). "GSAS II: the genesis of a modern open source all purpose crystallography software package," J. Appl. Crystallogr. **46**, 544–549.

Turner, M. J., McKinnon, J. J., Wolff, S. K., Grimwood, D. J., Spackman, P. R., Jayatilaka, D., and Spackman, M. A. (**2017**). *CrystalExplorer17* (University of Western Australia). Available at: http://hirshfeldsurface.net.

van de Streek, J., and Neumann, M. A. (**2014**). "Validation of molecular crystal structures from powder diffraction data with dispersion-corrected density functional theory (DFT-D)," Acta Crystallogr. B Struct. Sci. Cryst. Eng. Mater. **70**(6), 1020–1032.

Wang, C., Wang, J., and Chen, W. (**2007**). "Crystal structure and crystal habit prediction studies on ceftriaxone sodium," Chin. J. Antibiot. **32**, 672–678.

Wang, J., Toby, B. H., Lee, P. L., Ribaud, L., Antao, S. M., Kurtz, C., Ramanathan, M., Von Dreele, R. B., and Beno, M. A. (**2008**). "A dedicated powder diffraction beamline at the Advanced Photon Source: commissioning and early operational results," Rev. Sci. Instrum. **79**, 085105.

Wavefunction, Inc (**2018**). Spartan '18 Version 1.2.0, Wavefunction Inc., 18401 Von Karman Ave., Suite 370, Irvine CA 92612.

Yang, L., Lu, H., Yao, B., An, Z., Hao, J., Qi, Y., Li, J., Xu, Y., Yuan, J., Qi, G., and Hu, Y. (**2012**). "Crystal form of boceftriaxone sodium and preparation methods for crystal form," Chinese Patent CN102875574A.

Zhang, C., Wang, J., and Wang, Y. (**2005**). Non-isothermal dehydration kinetics of ceftriaxone disodium hemiheptahydrate," Ind. Eng. Chem. Res. **44**, 7057–7061.

https://doi.org/10.1017/S0885715620000299 Published online by Cambridge University Press